

Achieving optical gain in waveguide-confined nanocluster-sensitized erbium by pulsed excitation

Gerald M. Miller,^{a)} Ryan M. Briggs, and Harry A. Atwater

Thomas J. Watson Laboratories of Applied Physics, California Institute of Technology, Pasadena, California 91125, USA

(Received 15 March 2010; accepted 15 June 2010; published online 27 September 2010)

We use a rate equation approach to model the conditions for optical gain in nanocluster sensitized erbium in a slot waveguide geometry. We determine the viability of achieving net gain for the range of reported values of the carrier absorption cross section for silicon nanoclusters. After accounting for the local density of optical states modification of the emission rates, we find that gain is impossible in continuous wave pumping due to carrier absorption, regardless of the carrier absorption cross section. We, therefore, propose a pulsed electrical operation scheme which mitigates carrier absorption by taking advantage of the short lifetime of silicon nanoclusters compared to erbium. We show that pulsed excitation of a 10 nm layer achieves a modal gain of 0.9 dB/cm during each pulse. Furthermore this gain can be increased to 2 dB/cm by pumping a 50 nm layer. © 2010 American Institute of Physics. [doi:10.1063/1.3465120]

I. INTRODUCTION

In the pursuit of a silicon based near-infrared optical source, current research has focused heavily on silicon compatible materials such as silicon nanostructures and rare earth dopants. A great deal of research has focused on erbium as an optical dopant because it emits in the telecommunication band near 1.5 μm . In 1996, Fujii *et al.*¹ found that combining silicon nanocrystals with Er in an oxide matrix leads to a significant increase in the Er^{3+} photoluminescence intensity. It is now known that silicon nanoclusters (Si-nc) act as efficient sensitizers of Er^{3+} ions located nearby in the matrix. Specifically, the effective emission cross section of Er has been found to increase many orders of magnitude, from $\sigma_{\text{Er}} \sim 10^{-21} \text{ cm}^2$ in oxide to $\sigma_{\text{eff}} \sim 10^{-16} \text{ cm}^2$ when coupled to Si-ncs.

This led to research on Er doped Si nanocluster (Er:Si-nc) gain media. However, only one paper to the authors' knowledge has shown gain in this system.² Many mechanisms have been found that limit gain in this system, including Er concentration quenching,³ co-operative upconversion,^{4,5} and carrier absorption.^{5,6} The present paper is concerned with loss due only to carrier absorption, where light emitted by Er^{3+} is absorbed by excited carriers in the nanoclusters. The carrier absorption cross section of Si nanoclusters has been reported to have values of $\sigma_{\text{ca}} = 8 \times 10^{-17} \text{ cm}^2$ and $\sigma_{\text{ca}} = 4 \times 10^{-19} \text{ cm}^2$,^{6,7} for different nanocluster ensembles, and these two values straddle the line at which material gain is possible in Er:Si-nc bulk media.⁵

A promising device architecture for integrating an electrically driven light source on the complementary metal-oxide semiconductor platform is the slot waveguide, where a gain medium is placed between two silicon layers, which act as a waveguide while providing electrical access to the slot layer. While Er:Si-nc gain media are well described in bulk, the gain achievable in waveguide-based devices depends on

the device geometry and mode profile. The higher index silicon layers shorten the lifetime of emitters in the gain medium due to the increased local density of optical states (LDOS), described in Sec. III B. We find that gain in Er:Si-nc media incorporated in a slot waveguide is only possible using pulsed excitation, even if σ_{ca} is small enough to allow gain in bulk media under continuous-wave (CW) excitation.

II. RATE EQUATION MODELING

We develop here a rate equation model for the coupled Er:Si-nc system, both as a bulk medium and as the slot layer in a silicon slot waveguide. The energy level scheme is shown in Fig. 1, and the relevant parameters used in the calculation are listed in Table I.

The Si-nc is depicted as a two level system with energies E_b and E_a , having populations n_b and n_a , respectively. The Si-nc cross section is σ_{nc} , and the Si-nc lifetime, τ_{nc} , is geometry dependent.

The Er^{3+} ions are depicted as a three level system with energies E_3 , E_2 , and E_1 , having populations N_3 , N_2 , and N_1 , respectively, where the highest energy level, E_3 , is sensitized by the Si-ncs. The lifetimes of the various levels are τ_{21} , τ_{31} , and τ_{32} . Excitations of energy E_3 quickly decay to the first

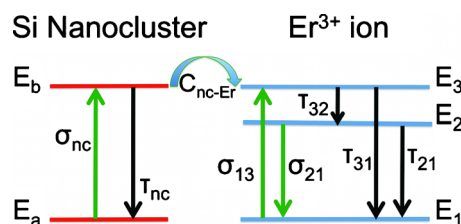


FIG. 1. (Color online) Energy levels of erbium and silicon nanoclusters (Si-nc) used for this work. Si-ncs are modeled as a two level system and the Er^{3+} as a three level system, where the ground state transition, $E_2 \rightarrow E_1$, emits at 1.5 μm . $C_{\text{nc-Er}}$ is the transfer coefficient between Si-ncs and Er^{3+} . Values for the lifetimes and cross sections are given in Table I.

^{a)}Electronic mail: geraldm@caltech.edu.

TABLE I. Rate equation parameters.

	Bulk	10 nm slot: optical pumping	10 nm slot: electrical pumping
$\tau_{nc}(\mu s)$	50	7.1	7.1
$\tau_{21}(ms)$	3	0.291	0.291
$C_{nc-Er}(cm^3 s^{-1})$	3×10^{-15}	3×10^{-15}	3×10^{-15}
$\sigma_{nc}(cm^2)$	10^{-16}	10^{-16}	10^{-14}
$\sigma_{13}(cm^2)$	10^{-19}	10^{-19}	...
$\sigma_{21}(cm^2)$	8×10^{-21}	8×10^{-21}	8×10^{-21}
$\tau_{32}(\mu s)$	2.38	2.38	2.38
$\tau_{31}(\mu s)$	714	714	714

excited level, E_2 , which decays to E_1 by emitting a photon near $1.5 \mu m$. The coupling coefficient between the excited nanocluster level and the highest Er^{3+} level is C_{nc-Er} , and is assumed independent of device geometry. The parameter $\phi(t)$ is the time-dependent pump flux. The rate equations used to describe this interaction are given below

$$\begin{aligned}
 \frac{dn_b}{dt} &= -\frac{n_b}{\tau_{nc}} + \sigma_{nc}\phi(t)n_a - C_{nc-Er}n_bN_1, \\
 \frac{dn_a}{dt} &= \frac{n_b}{\tau_{nc}} - \sigma_{nc}\phi(t)n_a + C_{nc-Er}n_bN_1, \\
 \frac{dN_3}{dt} &= -\frac{N_3}{\tau_{32}} - \frac{N_3}{\tau_{31}} + C_{nc-Er}n_bN_1 + \sigma_{13}\phi(t)N_1, \\
 \frac{dN_2}{dt} &= \frac{N_3}{\tau_{32}} - \frac{N_2}{\tau_{21}}, \\
 \frac{dN_1}{dt} &= \frac{N_2}{\tau_{21}} + \frac{N_3}{\tau_{31}} - C_{nc-Er}n_bN_1 - \sigma_{13}\phi(t)N_1. \quad (1)
 \end{aligned}$$

The decay rates for Er:Si-nc films have been measured for bulk media;^{3,8} and in the present work, the bulk Si-nc lifetime, τ_{nc} , is assumed to be $50 \mu s$, and the bulk Er^{3+} lifetime, τ_{21} , is assumed to be 3 ms. The nanocluster concentration is assumed to be $10^{19} cm^{-3}$, and the assumed Er concentration is $2 \times 10^{20} cm^{-3}$, chosen to be just below the onset of concentration quenching.³ The values for C_{nc-Er} , τ_{32} , and τ_{31} have been experimentally determined by Pacifici *et al.*⁵ Two pumping mechanisms are considered as follows: optical pumping at 488 nm with a photon flux of $10^{20} cm^{-2} s^{-1}$, which excites both Si-ncs and Er, and electrical pumping, which is assumed to only excite Si-ncs. Under optical pumping at 488 nm, the Er^{3+} absorption cross section is σ_{13} , which has also been determined experimentally.⁵

III. RESULTS

A. Excitation in bulk media

Using the present rate equation model for bulk media, it is possible to achieve over 90% inversion of the Er^{3+} using CW optical pumping. This model implicitly assumes that all the Er^{3+} ions are both active and coupled to Si-ncs. This coupling is an active area of experimental research.^{9,10} However, net gain in the system is only possible if gain from inverted Er^{3+} is greater than loss due to carrier absorption.

Here we define a figure of merit, χ , which is the ratio of gain due to inverted Er^{3+} to absorption by excited Si-ncs

$$\chi = \frac{g}{\alpha_{ca}} = \frac{\sigma_{21}(N_2 - N_1)}{\sigma_{ca}n_b}, \quad (2)$$

where σ_{21} is the emission cross section of Er^{3+} at $1.5 \mu m$, $N_2 - N_1$ is the inverted population of Er^{3+} ions, σ_{ca} is the absorption cross section of nanoclusters at $1.5 \mu m$, and n_b is the population of excited Si-ncs, which is 13% using this model. The Er^{3+} emission cross section at $1.5 \mu m$, $\sigma_{21} = 8 \times 10^{-21} cm^2$, comes from Mertens and Polman,¹¹ and is assumed to be the same as the absorption cross section at $1.5 \mu m$, σ_{12} . This number is more than an order of magnitude lower than that used by Pacifici,⁵ reflecting a newer experimental result.

If $\chi > 1$, then gain is possible in the system, whereas if $\chi < 1$, carrier absorption overwhelms gain from Er^{3+} . We find that $\chi < 1$ for all pump powers if the carrier absorption cross section found by Kekatpure and Brongersma,⁶ $\sigma_{ca} = 8 \times 10^{-17} cm^2$, is used. This is because even at close to 100% inversion, the excited nanoclusters are efficiently absorbing the Er^{3+} emission. However, if the carrier absorption cross section obtained by Navarro-Urrios *et al.*,⁷ $\sigma_{ca} = 4 \times 10^{-19} cm^2$, is used, we find that $\chi > 1$ for CW excitation. This is similar to a previous result from Pacifici *et al.*⁵

B. Excitation in slot waveguides

Recent work has explored using the Er:Si-nc system as a gain medium in silicon slot waveguides.¹²⁻¹⁴ In this geometry, shown in Fig. 2, a thin layer of active material exists between two silicon layers. The fundamental transverse-magnetic (TM) mode at 1535 nm is tightly confined to the slot layer, which increases the modal gain.¹⁵ The slot geometry could also allow electrical pumping of the thin dielectric active layer by doping the silicon cladding layers.¹⁴ Furthermore, resonators fabricated on the slot waveguide structure could allow for laser operation. Lastly, this geometry significantly modifies the LDOS of an emitter in the slot, which changes the emitter's radiative rate.^{12,16}

We model a slot waveguide with a 10 nm Er:Si-nc layer ($n=1.57$) between two 140 nm Si layers on SiO_2 (Fig. 2). This enables single TM mode operation of the waveguide, and uses an active layer thin enough to pump electrically via tunneling current. The LDOS enhancement of the radiative rate for both the Er^{3+} and Si-ncs was calculated for this structure, shown on the right in Fig. 2. At the Er^{3+} emission wave-

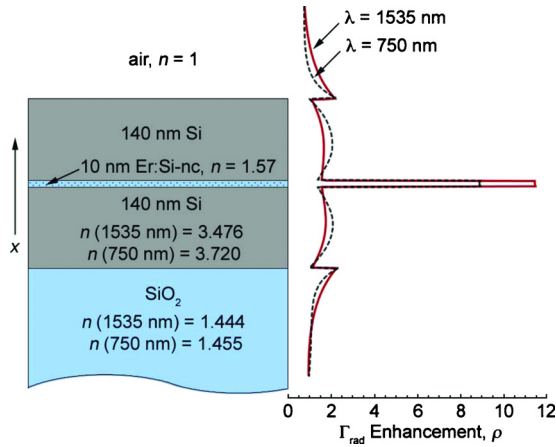


FIG. 2. (Color online) Radiative rate enhancement, ρ , in a slot waveguide as a function of position, at 1535 nm (red curve), and 750 nm (black dotted curve). The large average value of ρ in the slot leads to a large increase in the radiative rates of both the Si-ncs and Er^{3+} ions.

length of 1535 nm, the LDOS enhancement relative to bulk material with $n=1.57$ is more than 11, and at the nanocrystal emission wavelength of 750 nm, it is nearly 9. Details for this type of calculation can be found elsewhere.^{16,17} For these calculations, we use

$$\Gamma_{\text{tot}} = \rho \times \Gamma_{\text{rad}} + \Gamma_{\text{nrad}}, \quad (3)$$

where Γ_{tot} is the inverse of the total lifetime, Γ_{rad} is the radiative rate in bulk media, Γ_{nrad} is the decay rate due to nonradiative processes, and ρ is the calculated radiative rate enhancement factor due to the dielectric environment. For this structure, $\rho=11.43$ in the slot at 1535 nm (Fig. 2). For Er^{3+} in Si-rich oxide, a bulk radiative rate of 59 Hz is used, which is the rate found by de Dood and co-workers,¹⁸ corrected for the higher index of the layer. An assumed bulk nonradiative rate of 274 Hz gives the assumed bulk lifetime of 3 ms. We also assumed the nonradiative rate in the slot increases tenfold due to the presence of the silicon layers, consistent with experimental results.^{12,19} Therefore, $\Gamma_{\text{tot}}=3431$ Hz for Er^{3+} in a 10 nm slot.

A similar calculation was performed for the Si-ncs, using 9.4 kHz as both the bulk radiative rate and nonradiative rates in vacuum.⁸ At the peak emission wavelength of the nanoclusters, assumed to be 750 nm, $\rho=8.92$ (Fig. 2), and scaling the radiative rate by the index of the layer, $n=1.57$, a total rate of 141 kHz is obtained. This is a lifetime of 7.1 μs , which is still longer than the transfer time between the Si-ncs and Er, which is around 1 μs .⁵

Performing the rate equation analysis with these new rates shows that under optical pumping, inversion is only achievable for photon fluxes above $5.6 \times 10^{20} \text{ cm}^{-2} \text{ s}^{-1}$. However, in a slot waveguide geometry, electrical pumping is possible. Under electrical excitation, the Si-nc cross section increases by two orders of magnitude to $\sigma_{\text{nc}}=10^{-14} \text{ cm}^2$,²⁰ which increases the Er^{3+} effective cross section by the same factor. These calculations show 85% Er^{3+} inversion at 10 A/cm² of current density, while the excited nanocluster fraction increases to 74%. But due to the increased excited Si-nc fraction, $\chi < 1$ for all current densities. In fact, using the smaller value for σ_{ca} ,⁷ χ shows a maximum

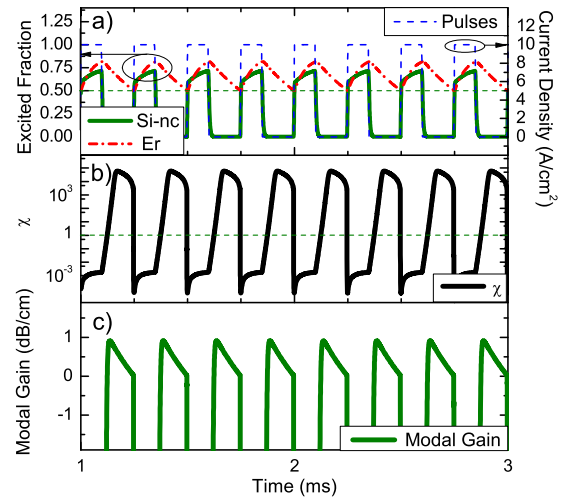


FIG. 3. (Color online) Pulsed electrical excitation of an Er:Si-nc slot. (a) Pulsed excitation (blue dotted curve) allows steady state inversion of the Er^{3+} (red dotted curve), while after each pulse the nanocluster excited fraction quickly approaches zero (green curve). (b) The ratio of gain to absorption, χ , is greater than one for a large part of each pulse. Gain from Er^{3+} overcomes carrier absorption loss as excited carriers in the nanoclusters recombine. (c) Modal gain in the slot waveguide reaches 0.9 dB/cm after each pulse.

of 0.6 at 2 A/cm² current density (not shown), implying that CW gain is impossible using electrical pumping. For currents greater than 2 A/cm², the increase in the excited Si-nc population is greater than the increase in the excited Er^{3+} population, decreasing the value of χ . A similar result is found under optical pumping, with χ showing a maximum of 0.6 at a photon flux of $1.2 \times 10^{21} \text{ cm}^{-2} \text{ s}^{-1}$, again implying gain is not achievable under CW excitation.

C. Pulsed excitation in slot waveguides

Here we propose a pulsed excitation scheme for inverting Er^{3+} . By pulsing the excitation, it is possible to invert the Er^{3+} during the excitation pulses, and Er^{3+} will remain inverted for some time after the pulse is turned off. Since $\tau_{21} \gg \tau_{\text{nc}}$, carriers in the Si-ncs will decay quickly and there will be a period of each excitation cycle where carrier absorption is thus very small.

Figure 3 shows the time dynamics of the Er:Si-nc system under pulsed 10 A/cm² pumping. The pulse rate is chosen to be 4 kHz, and the pulse length is 0.1 ms, hence the duty cycle is 40%. Pulsed electrical excitation is considered here, however the concept also applies to optical pumping if sufficiently high pump powers are available. Figure 3(a) shows the Er^{3+} and Si-nc excited fractions, plotted as a function of time with the pulse train. The Er^{3+} reaches inversion after very few excitation pulses and remains inverted in the steady state. However, the Si-nc excited fraction peaks around 0.7 and decays to near zero quickly once the pulse is turned off. Figure 3(b) is the figure of merit, χ , for this pulse train, plotted on a logarithmic scale as a function of time. Note this figure uses $\sigma_{\text{ca}}=8 \times 10^{-17} \text{ cm}^2$,⁶ which is the larger value, and results in increased loss. The figure of merit, χ , grows rapidly as the Si-nc population decreases, and stays above 1 for over 40% of the pulse period. During the fraction of the pulse cycle where $\chi > 1$, gain is possible because of the very

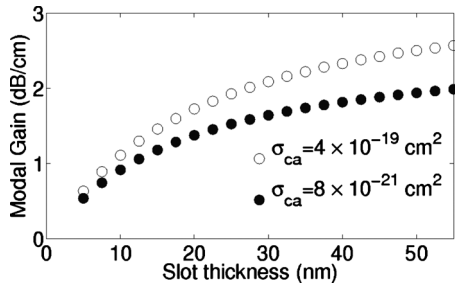


FIG. 4. Maximum gain for Er:Si-nc in a slot waveguide. As the slot thickness increases, more of the mode overlaps the active region, resulting in increased modal gain.

low loss due to carrier absorption. This pulsing scheme is also relatively insensitive to the value of σ_{ca} , because changing σ_{ca} only scales the value of χ , which is much greater than 1.

D. Modal gain

For the pulsing scheme described above, it is possible to calculate the modal gain for the fundamental TM mode of the structure described in Fig. 2. For light propagating in the z-direction, the modal gain coefficient, α_m , is given by the following expression:

$$\alpha_m = [\sigma_{21}(N_2 - N_1) - \sigma_{ca}n_b] \times \frac{\int_{\text{slot}} 2c\epsilon_0 n(x) \mathbf{E} \cdot \mathbf{E}^* dx}{\int_{-\infty}^{\infty} (\mathbf{E} \times \mathbf{H}^* + \mathbf{E}^* \times \mathbf{H}) \cdot \hat{\mathbf{z}} dx}. \quad (4)$$

The first term in Eq. (4) represents the sources of gain and loss in this system, assumed to be only gain from excited Er^{3+} and absorption from ground state Er^{3+} and excited carriers in Si-ncs. The second term is the modal confinement factor for the given geometry,²¹ where c is the speed of light, ϵ_0 is the permittivity of free space, $n(x)$ is the refractive index profile of the slot structure, \mathbf{E} is the electric field and \mathbf{H} is the magnetic field for a mode propagating in the z direction. This term is integrated over the Er:Si-nc slot, and for a 10 nm slot has a value of 0.285.

The result of this calculation for pulsed electrical excitation is given in Fig. 3(c). During each pulse the gain reaches a maximum of just over 0.9 dB/cm before decaying. Note that for this slot waveguide structure, gain is not achievable under CW pumping due to carrier absorption alone. This plot uses the larger value for σ_{ca} , but when using the smaller value, the two order of magnitude decrease in σ_{ca} only increases this peak value of gain to 1.1 dB/cm (Fig. 4). Because the Si-ncs decay faster than Er, carrier absorption is negligible shortly after the excitation pulse is turned off, which makes the modal gain relatively insensitive to the magnitude of σ_{ca} .

To achieve net gain in a waveguide with lateral confinement, this puts stringent requirements on the intrinsic waveguide loss. Passive Si waveguides have been fabricated with losses on the order of 0.4 dB/cm for TE modes and 1 dB/cm for TM modes.²¹ To achieve net gain and lasing, the modal gain in the TM mode must be at least 1 dB/cm to overcome waveguide losses alone. Practically, the modal gain must be

even larger than 1 dB/cm to overcome other sources of loss, such as loss due to integration of electrical contacts or cooperative upconversion in the Er:Si-nc layer. The simplest way to increase gain would be to increase the Er concentration, which was not done in this work to avoid the parasitic effect of concentration quenching. However, it is possible that improved thin film fabrication can lead to higher Er incorporation.¹⁰

Another way to increase gain is to make the active layer thicker. This allows the active layer to overlap a larger fraction of the confined TM mode, increasing the gain via the integral factor in Eq. (4), which increases from 0.285 for a 10 nm slot to 0.603 for a 50 nm slot. Figure 4 plots the maximum gain as a function of slot thickness for each value of σ_{ca} used in this work. The increase in gain is most pronounced at smaller thicknesses and saturates at larger thicknesses. For a 50 nm slot, the peak gain reaches 2 dB/cm for the higher value of σ_{ca} and 2.5 dB/cm for the lower value, which is a significant fraction of the theoretical maximum assuming complete inversion and zero carrier absorption, $\sigma_{21} \times N_{\text{Er}} = 6.95$ dB/cm. Despite the large difference in magnitude for the values of σ_{ca} , the difference of only 0.5 dB/cm again shows the insensitivity of the modal gain to the value of σ_{ca} in a pulsing scheme. A 10 nm thickness was chosen for this work with the intention of using tunnel injection as the pumping mechanism, however this need not be the case. It is possible that bipolar injection could be used to pump thicker layers.^{22,23}

For this calculation, contributions due to electrically excited carriers in the silicon have been neglected. For a background doping level of 10^{15} cm^{-3} , this introduces a negligible change in the index for our purposes. During the accumulation phase of the pulse, carriers in the silicon can reach very high levels; however, during these times carrier absorption in the Si-ncs is significant, so net gain is not achievable during this fraction of the excitation pulse.

IV. CONCLUSION

We have applied rate equation modeling to silicon slot waveguides using Er:Si-nc as the active media, and have determined that gain is likely not achievable under CW excitation due to carrier absorption by excited nanoclusters. However, using a pulsed injection scheme, it is possible to take advantage of the comparatively short excited state lifetime of Si-ncs and achieve gain in this system. With pulsed excitation, the modal gain in the Er:Si-nc slot waveguide can be in the dB/cm range, depending on slot thickness, and furthermore is comparatively insensitive to the value of σ_{ca} .

The LDOS effect in the slot waveguide has been characterized and incorporated into the model. For laser applications, the increased radiative rate of Er^{3+} raises the threshold for lasing and carrier absorption results in net material loss in CW operation. While CW gain may be possible in bulk layers if σ_{ca} is sufficiently small, layers in slot waveguides require pulsed excitation to achieve gain.

Aside from the significant problem of coupling a high fraction of Er to Si-ncs, all the other parameters in this paper have been chosen conservatively. There is no fundamental

barrier to the fabrication of films with lower nonradiative rates and higher active concentrations than those assumed here, which would only increase the gain in the Er:Si-nc slot waveguide system. The modal gain predicted here using pulsed excitation is slightly greater than passive Si waveguide losses that have been previously demonstrated, which is reason for optimism that net gain in a silicon based laser can be realized with this gain medium.

ACKNOWLEDGMENTS

The authors wish to thank D. Pacifici for many useful discussions. This project was funded by the AFOSR under the MURI Award No. FA9550-06-1-0470 and also under AFOSR Grant No. FA9550-06-1-0480. R.M.B. gratefully acknowledges the support of the National Defense Science and Engineering Graduate Fellowship.

- ¹M. Fujii, M. Yoshida, Y. Kanzawa, S. Hayashi, and K. Yamamoto, *Appl. Phys. Lett.* **71**, 1198 (1997).
²H. S. Han, S. Y. Seo, and J. H. Shin, *Appl. Phys. Lett.* **79**, 4568 (2001).
³F. Priolo, G. Franzo, D. Pacifici, V. Vinciguerra, F. Iacona, and A. Irrera, *J. Appl. Phys.* **89**, 264 (2001).
⁴E. Snoeks, G. N. van den Hoven, A. Polman, B. Hendriksen, M. B. J. Diemeer, and F. Priolo, *J. Opt. Soc. Am. B* **12**, 1468 (1995).
⁵D. Pacifici, G. Franzo, F. Priolo, F. Iacona, and L. D. Negro, *Phys. Rev. B* **67**, 245301 (2003).
⁶R. D. Kekatpure and M. L. Brongersma, *Nano Lett.* **8**, 3787 (2008).
⁷D. Navarro-Urrios, A. Pitani, N. Daldosso, F. Gourbilleau, R. Rizk, G. Pucker, and L. Pavesi, *Appl. Phys. Lett.* **92**, 051101 (2008).

- ⁸R. J. Walters, J. Kalkman, A. Polman, H. A. Atwater, and M. J. A. de Dood, *Phys. Rev. B* **73**, 132302 (2006).
⁹B. Garrido, C. Garcia, S.-Y. Seo, P. Pellegrino, D. Navarro-Urrios, N. Daldosso, L. Pavesi, F. Gourbilleau, and R. Rizk, *Phys. Rev. B* **76**, 245308 (2007).
¹⁰K. Hijazi, R. Rizk, J. Cardin, L. Khomenkova, and F. Gourbilleau, *J. Appl. Phys.* **106**, 024311 (2009).
¹¹H. Mertens and A. Polman, *Appl. Phys. Lett.* **86**, 241109 (2005).
¹²R. M. Briggs, G. M. Miller, and H. A. Atwater, *Proceedings of the Sixth IEEE International Conference on Group IV Photonics*, San Francisco, California (IEEE, New York, 2009), pp. 223–225.
¹³M. Galli, D. Gerace, A. Politi, M. Liscidini, M. Patrini, L. C. Andreani, A. Canino, M. Miritello, R. Lo Savio, A. Irrera, and F. Priolo, *Appl. Phys. Lett.* **89**, 241114 (2006).
¹⁴C. A. Barrios and M. Lipson, *Opt. Express* **13**, 10092 (2005).
¹⁵T. Robinson, K. Preston, O. Painter, and M. Lipson, *Opt. Express* **16**, 16659 (2008).
¹⁶Y. C. Jun, R. M. Briggs, H. A. Atwater, and M. L. Brongersma, *Opt. Express* **17**, 7479 (2009).
¹⁷H. P. Urbach and G. L. J. A. Rikken, *Phys. Rev. A* **57**, 3913 (1998).
¹⁸M. J. A. de Dood, L. H. Slooff, A. Polman, A. Moroz, and A. van Dlaenderen, *Phys. Rev. A* **64**, 033807 (2001).
¹⁹C. Creatore, L. C. Andreani, M. Miritello, R. Lo Savio, and F. Priolo, *Appl. Phys. Lett.* **94**, 103112 (2009).
²⁰F. Iacona, D. Pacifici, A. Irrera, M. Miritello, G. Franzo, F. Priolo, D. Sanfilippo, G. Di Stefano, and P. G. Fallica, *Appl. Phys. Lett.* **81**, 3242 (2002).
²¹R. Pafchek, R. Tummidi, J. Li, M. A. Webster, E. Chen, and T. L. Koch, *Appl. Opt.* **48**, 958 (2009).
²²R. J. Walters, G. I. Bourianoff, and H. A. Atwater, *Nature Mater.* **4**, 143 (2005).
²³A. Marconi, A. Anopchenko, M. Wang, G. Pucker, P. Bellutti, and L. Pavesi, *Appl. Phys. Lett.* **94**, 221110 (2009).